THE ASTROPHYSICAL JOURNAL, 388:561–578, 1992 April 1

PHOTON BUBBLES: OVERSTABILITY IN A MAGNETIZED ATMOSPHERE

JONATHAN ARONS
Department of Astronomy and Department of Physics, 601 Campbell Hall, University of California, Berkeley, CA 94720 and
Institute of Geophysics and Planetary Physics, Lawrence Livermore National Laboratory
Received 1991 July 1; accepted 1991 October 7

ABSTRACT

Linear stability theory is used to study the formation of "photon bubbles" in a convectively stable scattering atmosphere supported against gravity entirely by radiation pressure. A WKB analysis shows that internal waves in an isothermal magnetized atmosphere are overstable, when the magnetic pressure of a vertical magnetic field satisfies $B^2/8\pi > (M_0/2\gamma)p_{\rm rad}$. Here $M_0 \ll 1$ is the ratio of the sound crossing time to the photon diffusion time in the atmosphere and γ is the ratio of specific heats. The unstable waves are buoyant, rising with a group velocity $\sim c_0 M_0$, where c_0 is the isothermal sound speed, and have maximum growth rate $\sim kc_0 M_0^{0.4}$ when $kh \gg M_0^{-1/2}$. Here k is the wavenumber, and h is the isothermal scale height. The most unstable waves correspond to the formation of long vertical fingers of radiation where the density is depleted relative to the surroundings. The instability mechanism is the small conductive transfer of heat from high-density to low-density regions in the wave, while the wave's propagation is maintained by much larger radiative heat transfer across the magnetic field.

A simple model is developed for the two-dimensional structure of a plasma mound formed by laminar accretion onto the magnetic poles of a neutron star, in which upward photon diffusion balances downward photon advection with the plasma. It is shown that the vertical pressure and density structure is the same as in an isothermal atmosphere. Application of the stability theory to this model suggests photon bubbles would form in a polar accretion mound under the conditions expected in accretion-powered pulsars within a few tenths of a millisecond. Because long-wavelength modes have the largest rise speeds, eventual dominance by a few large bubbles is suggested, and possible connections between bubble formation and short-time variability in accretion-powered pulsars is briefly discussed, as well as a possible connection of the photon bubble phenomenon to the rapid time variability observed in the Rapid Burster and in quasi-periodic oscillator sources.

Subject headings: MHD — stars: atmospheres — stars: neutron

1. INTRODUCTION

Plasmas supported against gravity by radiation pressure occur in a variety of astrophysical contexts, most prominently in very hot stars and in accretion-powered X-ray sources, both of the Galactic and the extragalactic variety. In this paper, I derive the linear growth rate of a diffusive buoyancy instability in a radiation-supported atmosphere embedded in a strong vertical magnetic field. This instability may result in the formation of "photon bubbles," buoyant low-density regions within the atmosphere which might rise and "burst," leading to strong fluctuations in the radiative output from the system. This investigation was motivated by observations of photon bubbles in time-dependent numerical calculations of accretion onto the polar caps studies of magnetized neutron stars (Klein & Arons 1989, 1991, and 1992, in preparation), and I will choose the equilibrium model and the parameters of interest from this neutron star environment. Since photon bubbles may be of importance to a wide variety of radiatively supported systems, however, the instability is described in general terms.

The basic idea of the instability is as follows. Suppose we pretend that a small region forms with vertical size less than an atmospheric scale height with plasma density lower but radiation pressure higher than in the surroundings. Such a zone is buoyant and rises, with the buoyancy force balanced by the pressure gradient in the zone. New radiation diffuses in from the sides, and if the net flux is into the low-density region, the buoyancy will increase. It turns out that if the bubble is constrained to expand only in one dimension along the direction of gravity, the net flux is into the bubble and the motion is unstable, while if the bubble can expand freely in the sideways directions, the conductive increase of internal energy can be relaxed by adiabatic expansion and the net effect of radiation conduction is damping. We therefore expect to see instability on a time scale related to the rate at which radiation diffuses over a scale height, with the growth rate depending on the buoyancy force, and with growth occurring only when the density disturbance is confined in the direction across the flow. The constraint to one-dimensional motion along the vertical direction can be achieved only when there is a sufficiently strong vertical magnetic field. I will show that a magnetic field can be strong enough to allow the onset of photon bubbles, while still having a dynamically insignificant magnetic pressure with respect to the equilibrium structure of the medium.

Speculations on the formation of photon bubbles in a medium which is otherwise stable to convection have a long history. Prendergast & Spiegel (1973) first suggested that photon bubbles might form, reasoning by analogy to the behavior of fluidized beds. Spiegel (1976) outlined a simplified stability analysis with electron scattering as the only coupling between radiation and matter which suggested such bubbles might form in a static, unmagnetized exponential atmosphere supported by both radiation and gas pressure, and also described a simple model of a single bubble's rise, assuming they do form in the first place (Spiegel 1977). However, he chose an ordering in his stability analysis which led to the neglect of advection of radiative enthalpy. When the same

problem was fully investigated by Marzek (1977), only stable solutions were encountered, at least for radiative support below the Eddington limit. Since static equilibria exist only for a sub-Eddington radiation flux, these results do not address the existence of photon bubble instabilities in the super-Eddington environments sometimes encountered in accreting systems.

Studies of accretion-powered pulsars have led to suggestions that the radiation pressure support might lead to "turbulent" flow in the accretion mound formed just above the stellar surface (e.g., Basko & Sunyaev 1976). Because the magnetic field focuses the accreting plasma onto a small surface area, the effective Eddington limit for a 1 $M_\odot$ neutron star can be as small as $10^{35.5}$ ergs s^{-1} (Basko & Sunyaev 1976; Arons & Klein 1992, in preparation). Almost all the observed sources accrete at super-Eddington rates, as far as the low-altitude flow in the accretion column is concerned. Basko & Sunyaev's (1976) qualitative thought here was an analogy to the classical problem of Rayleigh-Taylor instability, since the "heavy" plasma is supported by the "light" photons. However, both their own model of the accretion column's structure, and one-dimensional calculations of super-Eddington accretion flow which do not impose an inverted density structure as an initial assumption (Klein, Stockman, & Chevalier 1980) show no signs of the inverted density or entropy needed to drive such unstable flow. This leads one to suspect that models which presume such inverted structure (e.g., Cowie, Ostriker, & Stark 1978; Demel, Morfill, & Atmanspacher 1990) in fact describe only an initial transient, which in the absence of other intrinsic instability would quickly relax to the stably stratified medium characteristic of model atmospheres for O stars, for example.

In addition, in the neutron star context, the strong magnetic field prevents the three-dimensional interchange motions which are part of the classical Rayleigh-Taylor instability. Instead, the required motions must be the lifting of plasma overlying buoyant regions, until eventually the radiation can leak out sideways and allow the plasma to settle down. Syrovatskii & Zhugzhda (1967) and Zhugzhda (1970) studied a fully compressible model of overstable convection in a strong magnetic field, in the context of sunspot models. They assumed an atmospheric model in which temperature increased linearly with height and found that radiative heat conduction causes the sound waves to become unstable. This kind of model has an inverted entropy gradient. In the specific context of accreting neutron stars, Hameury, Bonnazola, & Heyvaerts (1980) and Wang (1982) studied the linear growth of disturbances in a plane-parallel, static, optically thick layer supported by a combination of radiation and gas pressures. Hameury et al. (1980) chose an equilibrium in which the gas pressure and the density were both uniform, while the radiation pressure is a linear function of height, while Wang (1982) found an equilibrium which requires an external pressure above the layer to hold it in place. Both equilibria had inverted entropy gradients, and both investigations revealed instabilities based on buoyancy forces. However, I will show in § 3 that a reasonable equilibrium model for a polar accretion mound does *not* have an inverted entropy gradient, as is the case for the Basko & Sunyaev (1976) and Klein et al. (1980) models; of course, none of these models have inverted density gradients, as must be the case if they are in dynamical equilibrium (either static or steadily flowing). Wang's (1982) results suggest that the instability almost vanishes when the gas pressure support is negligible, as is the case in the polar mounds, a rather surprising conclusion considering the propensity of light fluids to escape from beneath overlying heavier ones. Furthermore, because the equilibria had nonconstant pressure scale height, the stability analyses required were very complex, employing numerical methods even for solution of the linear problem.

The possibility of photon bubble instabilities has been mentioned in other contexts. Lamb (1989), based on Spiegel's (1976, 1977) results, suggests that fluctuations in QPO sources might have their origin in photon bubbles forming in an accretion disk surrounding a weakly magnetized neutron star. Hogan (1991) has suggested a different instability driven by "mock gravity" in the early universe which might play a role in the formation of cosmological density inhomogeneities.

I carry out a WKB analysis of the stability of an exponential atmosphere in § 2, where I show that there is a diffusive buoyancy instability at short wavelength when the magnetic field is strong enough to restrict the plasma to motion only parallel to the magnetic field. In this $B = \infty$ limit, the instability appears in the entropy mode of the plasma. I also show that when the magnetic effects are absent, the instability disappears, with the buoyant pressure disturbances carried off as internal gravity waves. The instability is treated using ideal MHD for finite values of the magnetic field in the appendix. In § 3, I give a physical derivation of the equilibrium structure of a mound sitting at a magnetic pole of a steadily accreting neutron star. The basic point of this analysis is to motivate the use of an exponential atmosphere in an at least one astrophysical environment of interest. Several aspects of these results are discussed in § 4, including the estimation of a threshold value of the magnetic field, above which the instability is present. The application of these results to models of accreting neutron stars is also discussed in this section. My results are summarized in § 5.

2. OVERSTABILITY OF AN EXPONENTIAL ATMOSPHERE SUPPORTED BY RADIATION PRESSURE

Consider a plane-parallel layer of fully ionized plasma in hydrostatic equilibrium with the gravitational acceleration $g = -g\hat{z}$ directed downward along the z-axis with g = constant. Assume the gas pressure is negligible and the optical depth is large, so that the radiation force can be represented as the gradient of the isotropic equilibrium radiation pressure p_0. Finally, assume $\partial p_0/\partial \rho_0 \equiv c_0^2$ is a constant. Then the equation of hydrostatic equilibrium yields

$$p = p_* \exp(-z/h), \qquad \rho = \rho_* \exp(-z/h), \tag{1}$$

where the scale height is

$$h = \frac{g}{c_0^2}, \tag{2}$$

and p_* and ρ_* are constants. Finally assume the atmosphere is embedded in a uniform vertical magnetic field $\boldsymbol{B}_0 = B_0\hat{z}$. The presence of this field does not affect the equilibrium.

2.1. *Instability of the Atmosphere in a Superstrong Magnetic Field*

Now consider disturbances to this equilibrium, when the magnetic field is so strong that the plasma is constrained to move only along the magnetic field, with velocity $\boldsymbol{v} = v_1 \hat{\boldsymbol{z}}$. The equations of mass energy and momentum flux in the form I use them are derived and discussed by Arons, Klein, & Lea (1987), except for the effects of radiative viscosity. Including viscous stress due to isotropic scattering yields the linearized continuity and momentum equations

$$\frac{\partial \rho_1}{\partial t} = -\rho_0 \frac{\partial v_1}{\partial z} - v_1 \frac{\partial \rho_0}{\partial z} = -\rho_0 \frac{\partial v_1}{\partial z} + \rho_0 \frac{g}{c_0^2} v_1 , \tag{3}$$

$$\frac{\partial v_1}{\partial t} = -\frac{1}{\rho_0}\frac{\partial p_1}{\partial z} - \frac{\rho_1}{\rho_0} g + \frac{\partial}{\partial z}\frac{4}{3}\mu_0 \frac{\partial v_1}{\partial z} , \tag{4}$$

while the linearized energy equation is

$$\begin{aligned}\frac{\partial p_1}{\partial t} &= -v_1 \frac{\partial p_0}{\partial z} - \gamma p_0 \frac{\partial v_1}{\partial z} + \nabla \cdot \left[D_0 \nabla p_1 - D_0 \frac{\rho_1}{\rho_0} \nabla p_0 \right] \\ &= -\gamma p_0 \frac{\partial v_1}{\partial z} + \rho_0 g v_1 + D_0 \nabla_\perp^2 p_1 + \frac{\partial}{\partial z}\left[D_0 \left(\frac{\partial p_1}{\partial z} + \rho_1 g \right) \right] \\ &= -\gamma p_0 \frac{\partial v_1}{\partial z} + \rho_0 g v_1 + D_0 \nabla^2 p_1 + \frac{D_0 g}{c_0^2}\frac{\partial p_1}{\partial z} + D_0 g \frac{\partial \rho_1}{\partial z} + D_0 N_0^2 \rho_1 .\end{aligned} \tag{5}$$

In equation (5),

$$N_0 = \frac{c_0}{h} = \frac{g}{c_0} , \tag{6}$$

is closely related to the Brunt-Väissala frequency of the atmosphere. The quantity N_0^{-1} is the time it takes a signal traveling at the speed c_0 to cross the scale height h. I assumed the radiation has an isotropic diffusion coefficient dependent on density alone, as is the case when the diffusive process is Thomson scattering and

$$D = \frac{cm}{\rho \sigma_T} = c\lambda , \tag{7}$$

where σ_T is the Thomson cross section and λ is the mean free path. This assumption corresponds to the cyclotron energy $\hbar e B_0/m_e c$ being small compared to $2.8kT_\gamma$, where T_γ is the photon temperature. In stronger field environments, the scattering opacity becomes dependent on the temperature also, a case which I will not discuss further here. I included the viscous stress caused by radiative viscosity in (4). For isotropic Thomson scattering,

$$\mu_0 = \frac{4}{5}\frac{p_0 D_0}{c^2} \tag{8}$$

(Thomas 1930; Weinberg 1971). A detailed treatment of radiative viscosity actually requires a much more complex description (Mihalas & Mihalas 1984), but since the effects of viscosity turn out to be small, the simple Newtonian model used here will suffice.

2.1.1. *Low-frequency Diffusion Waves—A Simple Model*

Before solving the full equations, it is helpful to give a simpler physical model that captures the essential physics of the low-frequency diffusion wave which is destabilized by radiation pressure. The atmosphere has two characteristic time scales determined by the scale height h. The first is the time it takes a sound wave to cross a scale height,

$$t_s = h/c_0 = N_0^{-1} . \tag{9}$$

The second is the time taken by radiation to diffuse across the same length,

$$t_d = \frac{h^2}{D_0} = \frac{t_s}{M_0} , \tag{10}$$

where

$$M_0 \equiv \frac{D_0}{h^2 N_0} = \frac{c}{c_0 \tau_h} , \tag{11}$$

and $\tau_h \equiv \rho_0 \sigma_T h/m$ is the scattering optical depth through one scale height of the atmosphere. In most circumstances of interest, $M_0 \ll 1$ and the radiation diffusion time is much longer than the sound crossing time.

2.1.1.1. Heat Diffusion Waves

Suppose this relative ordering of the time scales also applies to our short-wavelength oscillations. Approximate hydrostatic equilibrium is established in a few sound crossing times. Once this is so, the pressure gradient acts to restore the positions of fluid elements displaced by the buoyancy force $-\rho_1 g$, by the inertial force $-\rho_0 \partial v_1/\partial t$ and the viscous force. When the period of the wave

is much longer than the acoustic time for a given wavelength, I approximate the momentum equation by assuming buoyancy provides *all* the displacement force; in normal stellar atmospheres, this balance of forces accurately describes the internal gravity waves, or g-modes, as I will recover below. Neglecting the inertial and viscous forces in equation (4) yields

$$\frac{\rho_1}{\rho_0} = -\frac{1}{g\rho_0}\frac{\partial p_1}{\partial z}. \tag{12}$$

The gradients in the equilibrium density are negligible, to zeroth-order in $(kh)^{-1}$, so the continuity equation combined with equation (12) yields

$$\frac{\partial v_1}{\partial z} = -\frac{1}{\rho_0}\frac{\partial \rho_1}{\partial t} = \frac{1}{g\rho_0}\frac{\partial^2 p_1}{\partial t\,\partial z}. \tag{13}$$

Integration of equation (13) with respect to z yields

$$v_1 = \frac{1}{g\rho_0}\frac{\partial p_1}{\partial t} \tag{14}$$

to zeroth-order in $(kh)^{-1}$.

The energy equation (5) then shows that the perturbed pressure is constant following the motion, $\partial p_1/\partial t + v_1\,\partial p_0/\partial z = 0$. If a fluid element moves up and down, the internal energy changes only from the gravitational work done. If the motion were simply the rise and fall of an incompressible body, this simple mechanical change in the internal energy would be the complete description of the internal energy changes. However, in general $\partial v_1/\partial z \neq 0$, and the volume of a fluid element changes as it moves, causing adiabatic work to be done on the gas and the photons. The energy equation then reduces to

$$-\gamma p_0 \frac{\partial v_1}{\partial z} + D_0 \nabla_\perp^2 p_1 = 0, \tag{15}$$

showing that the resulting adiabatic work then must be exactly balanced by diffusion of radiative energy in the *transverse* direction. This curious result occurs because when the radiation pressure and the gravitational forces are exactly balanced, the vertical diffusion flux vanishes:

$$q_\parallel = -D_0\left(\frac{\partial p_1}{\partial z} - \frac{\rho_1}{\rho_0}\frac{\partial p_0}{\partial_z}\right) = -D_0\left(\frac{\partial p_1}{\partial z} + \rho_1 g\right) = 0 \tag{16}$$

and all that is left of the radiation diffusion in the energy flow is diffusion across the gravitational field. Upon substitution of equation (13) into equation (15), I find

$$\frac{\partial^2 p_1}{\partial t\,\partial z} = \frac{gD_0}{\gamma c_0^2}\nabla_\perp^2 p_1 = c_0\frac{M_0}{\gamma}\nabla_\perp^2 p_1. \tag{17}$$

The physics of the wave motions contained in equation (17) can be understood from the following elementary solution. Suppose

$$p_1 = \alpha \sin\left[k_\parallel(z - v_p t)\right] \sin\left(\frac{\pi x}{L_\perp}\right) = \alpha \sin\left(\frac{\pi x}{L_\perp}\right)\mathscr{R}\exp\left\{i[k_\parallel(z - v_p t) - \pi/2]\right\} \tag{18}$$

for $0 < x < L_\perp$, with $p_1 = 0$ elsewhere. The quantities $k_\parallel$, α and v_p are constants. This heat wave propagating along the magnetic and gravitational fields is a solution of equation (17) if an only if the phase velocity is

$$v_p = -c_0\frac{M_0}{\gamma}\left(\frac{\pi}{k_\parallel L_\perp}\right)^2, \tag{19}$$

corresponding to the dispersion relation

$$\omega \equiv k_\parallel v_p = -k_\parallel c_0\frac{M_0}{\gamma}\left(\frac{\pi}{k_\parallel L_\perp}\right)^2 = -\frac{\pi^2}{\gamma}\frac{D_0}{L_\perp^2}\frac{1}{k_\parallel h} = -\frac{\pi^2}{\gamma}\frac{1}{t_d(L_\perp)}\frac{1}{k_\parallel h}, \tag{20}$$

where $t_d(L_\perp)$ is the diffusion time for heat to flow through the width of the wave. The transverse heat flux is

$$q_\perp = -D_0\frac{\pi}{L_\perp}\alpha \sin\left[k_\parallel(z - v_p t)\right]\cos\left(\frac{\pi x}{L_\perp}\right). \tag{21}$$

As shown in Figure 1, this tranverse heat flux carries heat out from regions of high radiation energy density into the surroundings, while it carries heat from the surroundings into the regions of low energy density. As a propagating peak of pressure arrives, the adiabatic work done is conducted out, while as a pressure peak leaves, the heat leaks back in just fast enough to restore the head of pressure driving the wave. Notice that the group velocity

$$v_g = \frac{\partial\omega}{\partial k_\parallel} = c_0\frac{M_0}{\gamma}\left(\frac{\pi}{k_\parallel L_\perp}\right)^2 \tag{22}$$

is always positive—the pressure wave (eq. [18]) rises, as one would expect since buoyancy is the basic driving force.

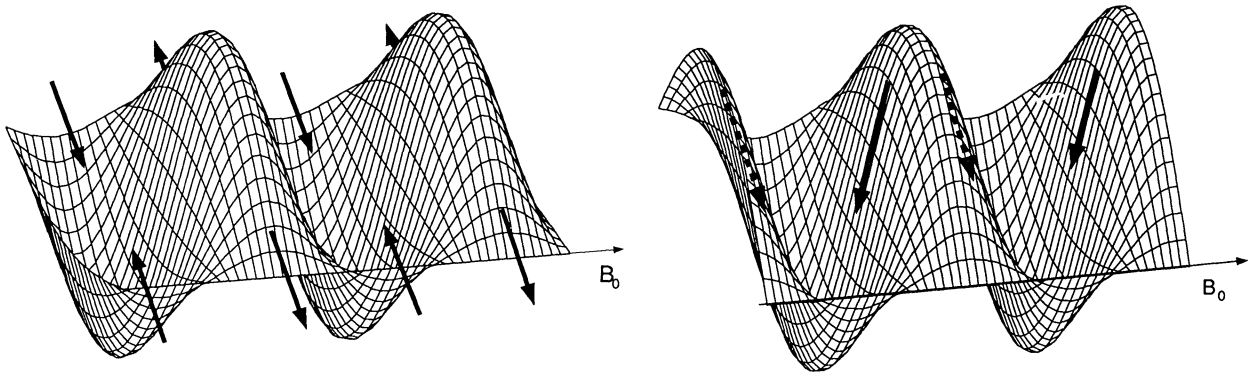

FIG. 1.—Pressure and density distributions of a buoyant entropy mode, confined between transverse dimensions $x = 0$ and $x = L_\perp$. *Left panel*: pressure distribution, with arrows showing the basic radiative heat flow into and out of the surroundings which supports the wave propagation. *Right panel*: density distribution, with arrows showing the small heat flow along the magnetic field which drives the wave unstable.

The sound crossing time for this wave, $t_s(k) = (kc_s)^{-1}$, is always short compared to the oscillation time, since

$$t_s(k)/t_{\rm wave}(k) = |\omega/k_\parallel c_s| = (M_0/\gamma^{3/2})(\pi/k_\parallel L_\perp)^2 .$$

Therefore, my assumption of hydrostatic equilibrium in the wave is well justified.

2.1.1.2. Parallel Heat Flux—The Instability Mechanism

Of course, the inertia is small, but not zero. Therefore, exact balance of the buoyancy force by the parallel pressure gradient is not strictly correct and the parallel heat flux is not exactly zero. However, since hydrostatic equilibrium is approximately valid, I can use the velocity found in equation (14) to evaluate the parallel heat flux from the momentum equation. Since $q_\parallel = -D_0(\partial p_1/\partial z + \rho_1 g)$, the momentum equation (4) yields

$$q_\parallel = \frac{D_0}{g}\left(\frac{\partial^2 p_1}{\partial t^2} - \frac{4}{3}\nu_0 \frac{\partial^3 p_1}{\partial^2 z\,\partial t}\right), \tag{23}$$

where

$$\nu_0 = \frac{\mu_0}{\rho_0} = \frac{4}{5}\left(\frac{c_0}{c}\right)^2 D_0 \tag{24}$$

is the kinematic viscosity. As will be shown below, the viscosity is unimportant in comparison to the fluid's inertia. In order of magnitude,

$$\frac{q_\parallel}{q_\perp} \sim \frac{\omega^2}{(\pi g/L_\perp)} = \frac{\pi}{\gamma^2}\frac{c}{c_0}\frac{\lambda_0}{L_\perp}\left(\frac{\pi}{k_\parallel L_\perp}\right)^2 . \tag{25}$$

Since the mean free path λ_0 must be small compared to the width of the wave for this fluid model to apply at all, and $M_0 = t_s(h)/t_d(h) \ll 1$, $q_\parallel/q_\perp \ll 1$ under most circumstances of interest.

The sense of the small parallel heat flux obtained from equation (23) is also shown in Figure 1, along with the mass density disturbance which accompanies the pressure wave. *The sense of the parallel heat flow is always to carry heat from the high-density regions of the wave to the low-density regions. Since the buoyancy is increased by the deposition of extra radiative energy in regions of lowered density, the amplitude of the wave systematically increases.* This is the mechanism of instability. The formation of regions of ever-increasing pressure but ever-decreasing density implies the formation of photon bubbles, regions in which the density goes essentially to zero, a conclusion consistent with detailed numerical simulations (Klein & Arons 1989, 1991).

An estimate of the growth rate can be obtained by using the parallel heat flux (eq. [23]) in the energy equation while continuing to neglect the comoving changes in the internal energy. Then equation (17) becomes

$$\frac{\partial^2 p_1}{\partial t\,\partial z} = \frac{gD_0}{\gamma c_0^2}\nabla_\perp^2 p_1 - \frac{D_0}{g}\left(\frac{\partial^3 p_1}{\partial z\,\partial t^2} - \frac{4}{3}\nu_0\frac{\partial^4 p_1}{\partial^3 z\,\partial t}\right). \tag{26}$$

Now the pressure wave (eq. [18]) yields the dispersion relation for the frequency $\omega \equiv k_\parallel v_p$,

$$\begin{aligned}\frac{\omega}{N_0} &= -\frac{M_0}{\gamma}\frac{k_\parallel h}{1 + (16/15)(k_\parallel \lambda_0)^2}\left(\frac{\pi}{k_\parallel L_\perp}\right)^2 + i\frac{M_0}{\gamma[1 + (16/15)(k_\parallel \lambda_0)^2]}\left(\frac{\omega}{N_0}\right)^2 \\ &\approx -\frac{M_0}{\gamma}\frac{k_\parallel h}{1 + (16/15)(k_\parallel \lambda_0)^2}\left(\frac{\pi}{k_\parallel L_\perp}\right)^2 + i\left(\frac{M_0}{\gamma}\right)^3 \frac{(k_\parallel h)^2}{[1 + (16/15)(k_\parallel \lambda_0)^2]^3}\left(\frac{\pi}{k_\parallel L_\perp}\right)^4 .\end{aligned} \tag{27}$$

The approximate result for ω assumes $\omega/N_0 \ll 1$.

Both the inertial force and the viscous force contribute to the departures from hydrostatic equilibrium which lead to the existence of the parallel heat flux. The term $16(k_\parallel \lambda_0)^2/15$ appearing in equation (27) represents the relative magnitude of the energy changes due to the part of the parallel heat flux coming from the viscous departures from mechanical equilibrium. For wavelengths long compared to the mean free path, these viscous contributions are always small. By contrast, the inertial departures from equilibrium yield weak overstability, as is expected from the qualitative argument above.

2.1.2. *Dispersion Relation Including Gradients*

The derivation of the frequency and growth rate (eq. [27]) has been quite cavalier, however, since in its derivation I have taken the equilibrium density to be constant whenever it appears inside a spatial derivative, and I have persisted in assuming the comoving changes in the internal energy are absent. Both assumptions are true to lowest order in $(k_\parallel h)^{-1}$, but the result yields a growth rate $\propto h^{-2}$. Thus, greater care is needed, in order to confirm the existence of overstability.

I assume the disturbances have short vertical wavelength, with

$$\begin{pmatrix} \rho_1 \\ v_1 \\ p_1 \end{pmatrix} = \begin{bmatrix} \tilde{\rho}(z) \\ \tilde{v}(z) \\ \tilde{p}(z) \end{bmatrix} \exp\left\{ i\left[\boldsymbol{k}_\perp \cdot \boldsymbol{r}_\perp - \omega t + \int^z dz' k_\parallel(z') \right] \right\}, \tag{28}$$

where $\boldsymbol{k}_\perp = k_x \hat{\boldsymbol{x}} + k_y \hat{\boldsymbol{y}}$, $\boldsymbol{r}_\perp = x\hat{\boldsymbol{x}} + y\hat{\boldsymbol{y}}$ with k_x and k_y both constant. The short-wavelength assumption is $k_\parallel h \gg 1$, and $k_\parallel$, $\tilde{\rho}$, $\tilde{v}$, $\tilde{p}$ all vary slowly, changing only on the length scale set by h.

I neglect radiative viscosity, since I found above that it does not affect the slow heat diffusion waves when the fluid approximation is valid. Upon substituting equation (28) into the linearized continuity and momentum equations (3) and (4), I find

$$\frac{\tilde{\rho}_1}{\rho_0} = \frac{k_\parallel^2 c_0^2 + i\Gamma_g^2}{\omega^2 + i\Gamma_g^2 - N_0^2} \frac{\tilde{p}_1}{p_0}, \qquad \tilde{v}_1 = c_0 \frac{\omega k_\parallel c_0}{\omega^2 + i\Gamma_g^2 - N_0^2} \frac{\tilde{p}_1}{p_0}, \tag{29}$$

while from equation (5),

$$\frac{\tilde{p}_1}{p_0} = \left(1 + i\frac{\Gamma_d}{\omega} + M_0 k_\parallel h \frac{N_0}{\omega}\right)^{-1} \left[\left(\frac{ig}{\omega c_0^2} + \gamma \frac{k_\parallel}{\omega} \right) \tilde{v}_1 + \frac{iD_0}{\omega c_0^2} (N_0^2 + i\Gamma_g^2) \frac{\tilde{\rho}_1}{\rho_0} \right]. \tag{30}$$

Here

$$\Gamma_d \equiv k^2 D_0 \tag{31}$$

is the diffusive damping rate of a mode of total wavenumber $k = (k_\parallel^2 + k_\perp^2)^{1/2}$, $\Gamma_g = (k_\parallel g)^{1/2}$ is the buoyancy rate, such that the velocity of rise of a free buoyant fluid element would be $\Gamma_g/k_\parallel$.

Simultaneous solution of equations (29) and (30) yields the dispersion relation

$$\frac{k_\parallel^2 c_s^2 + N_0^2}{\omega^2} - i\frac{k^2 D_0}{\omega} - \frac{k_\parallel g D_0}{c_0^2 \omega} + i\frac{k_\perp^2 D_0 N_0^2}{\omega^3} + \frac{k_\perp^2 D_0 k_\parallel g}{\omega^3} = 1. \tag{32}$$

Normalization of the frequency to N_0 yields the dispersion relation (32) in the form

$$\left(\frac{\omega}{N_0}\right)^3 + M_0(kh)^2\left(i + \frac{\mu}{kh}\right)\left(\frac{\omega}{N_0}\right)^2 - (1 + \gamma\mu^2 k^2 h^2)\frac{\omega}{N_0} - M_0(kh)^2(1-\mu^2)(kh\mu + i) = 0. \tag{33}$$

2.1.3. *Ideal Acoustic-Gravity Waves*

Suppose diffusion is negligible. Then $M_0 = 0$ and the solutions of equation (33) are

$$\omega^2 = N_0^2 + k_\parallel^2 c_s^2, \tag{34}$$

$$\omega = 0. \tag{35}$$

Here $c_s = \gamma^{1/2} c_0$ is the adiabatic sound speed. Equation (34) describes one-dimensional sound waves which carry energy exactly along the magnetic field, since the strong field prevents sideways oscillation. These are the one-dimensionalized analogs of the p-modes familiar in stellar atmospheres. When $k_\parallel h \gg 1$, as is required in deriving equation (34), the sound waves have frequencies high compared to N_0. If the limit $k_\parallel h \ll 1$ were permitted by the WKB approximation, equation (34) would imply the transformation of a sound wave into a neutrally stable, nonpropagating buoyancy oscillation at long wavelength. This is a correct conclusion, but can only be proved by solving the equations of motion without making the WKB assumptions.

Equation (35) is the dispersion relation of the entropy mode, when the motion is adiabatic. This is the wave which is destabilized by the combination of radiation diffusion and buoyancy. Internal gravity waves (the g-modes) are absent from this analysis, since they exist only if the plasma can move in the direction perpendicular to g. However, this zero frequency mode becomes the internal waves when motions in the transverse direction become significant.

2.1.4. *Radiative Buoyancy Instability—Photon Bubbles*

Now consider the full dispersion relation (33) but assume the diffusion time across a scale height is long compared to the sound crossing time through a scale height, $M_0 \ll 1$. If $k_\parallel h$ is not too large (eq. [33]) an approximate analytic solution can be found for weakly damped acoustic gravity waves with $|\omega|/N_0 \gg 1$. The approximate dispersion relation is obtained by neglecting the last

term of equation (33). Such neglect is equivalent to assuming the diffusion coefficient depends only on the unperturbed density and therefore that the parallel heat flux is simply $q_{\parallel} = -D_0 \partial p_1/\partial z$. From the discussion of the simple model, this is so only when the inertial force on the wave is large compared to the buoyancy force $-\rho_1 g$, as is appropriate for the high-frequency sound waves. The result is

$$\omega^2 + i\Gamma_d \omega - (k_{\parallel}^2 c_s^2 + N_0^2) = 0 , \tag{36}$$

whole solutions are

$$\omega \simeq -i\frac{\Gamma_d}{2} \pm (N_0^2 + k_{\parallel}^2 c_s^2)^{1/2}\left[1 - \left(\frac{M_0 kh}{2\mu}\right)^2\right], \tag{37}$$

showing the weak damping of the sound waves. If radiative viscosity is included, the damping rate is increased by a factor $1 + (4/5)(c_0/c)^2$. Syrovatskii & Zhugzhda (1968) concluded that sound waves in a stratified atmosphere immersed in a strong, vertical magnetic field become unstable with respect to oscillatory convection only if the ratio of specific heats exceeds approximately 1.2. The atmosphere analyzed here is isothermal, so one expects stability from their criterion, as is found.

A similar approximate result for the entropy mode with $|\omega|/N_0 \ll 1$ can be found by neglecting the term in ω^3 in (33), which had its origin in the inertial force in the momentum equation. The result for the entropy mode is then

$$\omega \simeq -\Gamma_d \frac{\Gamma_g^2}{N_0^2 + k_{\parallel}^2 c_s^2} - i\Gamma_d \frac{N_0^2}{N_0^2 + k_{\parallel}^2 c_s^2} + i\Gamma_d\left(\frac{\Gamma_d}{N_0}\right)^2 k_{\parallel}^2 h^2\left(\frac{N_0^2}{N_0^2 + k_{\parallel}^2 c_s^2}\right)^3\left(1 - \frac{k_{\parallel}^2}{k^2}\right)^2 . \tag{38}$$

A more useful form of equation (38) for numerical purposes is

$$\frac{\omega}{N_0} \simeq -M_0 \frac{(kh)^3}{1 + \gamma(kh\mu)^2}\mu(1 - \mu^2) - iM_0 \frac{(kh)^2}{1 + \gamma(kh\mu)^2}(1 - \mu^2) + iM_0^3 \frac{(kh)^8}{(1 + \gamma k^2 h^2 \mu^2)^3}\mu^2(1 - \mu^2)^2 . \tag{39}$$

where $\mu = \cos\theta = k_{\parallel}/k$. Both equations (38) and (39) show that this propagating entropy mode exists only if both diffusion and buoyancy effects are present, since the parallel heat flux becomes small and destablilizing only if the pressure gradient in the wave is in almost exact balance with the buoyancy forces. Equation (39) also shows that there is a threshold for overstability: the wavenumber must satisfy

$$kh > \frac{\gamma}{M_0}\cot\theta , \tag{40}$$

if there is to be growth. Below this threshold, radiative diffusion damps the wave, while well above threshold, the growth rate predicted by this analytic formula is

$$\Gamma \approx N_0\left(\frac{M_0}{\gamma}\right)^3 (kh)^2 \tan^4\theta, |\cos\theta| \gg (kh)^{-1} . \tag{41}$$

The much larger real part of the frequency is

$$\omega \approx -N_0 \frac{M_0}{\gamma} kh \frac{\sin^2\theta}{\cos\theta} , \tag{42}$$

in complete agreement with equation (20) if $k_{\perp}$ is identified with $\pi/L_{\perp}$. The threshold and the difference between the growth rate in equations (41) and the results of the simple model in equation (27) are both the consequence of the nonvanishing of the comoving internal energy changes to higher order in $(k_{\parallel} h)^{-1}$—for long wavelengths, the parallel heat flux is unimportant compared to the comoving change of the internal energy, which does not vanish to first order in $(k_{\parallel} h)^{-1}$.

2.1.5. *Numerical Growth Rates*

Unfortunately, once the wavenumber satisfies the threshold condition (40), the frequency is no longer small compared to N_0. Therefore, the dispersion relation (33) must be solved numerically. Examples of the solutions are shown in Figure 2, for the cases $M_0 = 0.1, 0.01$. Maximum growth occurs for propagation almost across the magnetic field, as $M_0 \to 0$. The maximum growth rate is shown in Figure 3.

The threshold condition (eq. [40]) and the real part of the frequency (eq. [42]) are both good descriptions of the numerical results. When the threshold condition is satisfied, growth occurs only for $kh \gg 1$, and the numerical results for the growth rate can be represented by

$$\Gamma_{\text{numerical}} \approx N_0 M_0^{0.4} \frac{k^3 h^3}{(1 + \gamma k^2 h^2 \mu^2)^{2.725}}\mu^2(1 - \mu^2)^2 , \tag{43}$$

along the ridge of maximum growth rate shown in Figure 2. As a function of the angle between the wave vector and the vertical, the growth rate (eq. [43]) maximizes at θ_m, with

$$\cos\theta_m = \frac{0.66}{kh} . \tag{44}$$

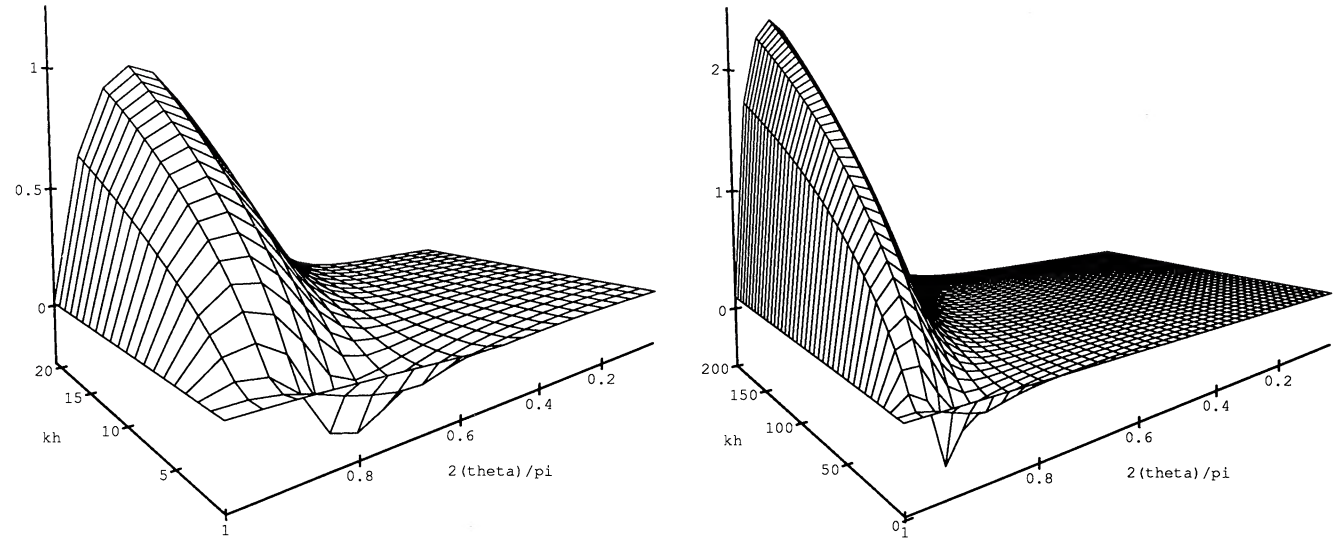

FIG. 2.—Growth rate of the photon bubble instability. *Left panel*: $M_0 = t_s(h)/t_d(h) = 0.1$. *Right panel*: $M_0 = 0.01$. The vertical axes give the growth rates measured in units of $N_0 = c_s/h$, plotted as a function of the total wavenumber k (measured in units of h^{-1}) and the angle the wavevector makes to the vertical θ (measured in units of $\pi/2$). As the diffusion time becomes long compared to the sound crossing time (decreasing M_0), the instability becomes almost entirely transverse, suggesting the growth of bubble structures elongated parallel to the magnetic field.

The maximum growth rate can be represented by

$$\Gamma_{\max} \approx N_0 M_0^{0.4} kh \,, \tag{45}$$

when $kh \gg 0.94/\sqrt{M_0}$. When $M_0 \ll 1$, the bubbles become very elongated, with $\cos\theta_m \ll 0.7\sqrt{M_0}$.

2.2. *Damped p- and g- modes in a Three-dimensional Atmosphere*

The unstable entropy wave studied in the previous section is closely related to the internal gravity modes of an unmagnetized atmosphere. Consider the propagation of short-wavelength waves with frequencies small compared to the frequencies of sound waves with the same wavelength. Furthermore, assume the restoring force is entirely gravitational. The fluid equations describing this simplified model are

$$\nabla \cdot \boldsymbol{v} = 0 \,, \qquad \frac{\partial \rho_1}{\partial t} - v_{\parallel} \frac{\rho_0}{h} = 0 \,, \qquad 0 = -\frac{\partial p_1}{\partial z} - \rho_1 g \,, \qquad \rho_0 \frac{\partial v_{\perp}}{\partial t} = -\nabla_{\perp} p_1 \,. \tag{46}$$

Traveling waves of the form of equation (28) yield the dispersion relation

$$\omega^2 = N_0^2 \tan^2\theta \rightarrow N_0^2 \left(1 - \frac{1}{\gamma}\right) \sin^2\theta \,, \tag{47}$$

where the second form is the well-known result when compressibility ($\gamma < \infty$, $\nabla \cdot \boldsymbol{v}_{\perp} \neq 0$) and inertia along the direction of gravity ($\tan^2\theta \rightarrow \sin^2\theta$) are included. Clearly, the internal waves are related to the unstable one-dimensional entropy mode, in the sense that buoyancy is the restoring force for both. In contrast to the one-dimensional entropy mode, the internal wave is close to incompressible, with $(\nabla \cdot \boldsymbol{v})/(\partial v_{\parallel}/\partial z) \approx (kh)^{-1} \ll 1$—adiabatic compressions parallel to gravity are balanced by adiabatic decom-

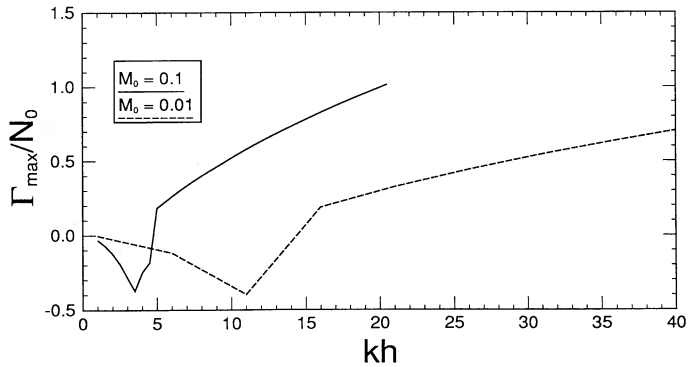

FIG. 3.—Maximum growth rate of the photon bubble instability, for $M_0 = 0.1, 0.01$

pression due to the sideways motion across $\boldsymbol{g}$, not by heat conduction. When $M_0 \ll 1$, the effect of heat conduction should be simply to reduce the entropy content of an internal wave, i.e., act solely to damp the motion. This can be shown by considering the full dispersion relation for internal waves, including radiative heat conduction.

The motions are three-dimensional, with linearized continuity equation

$$\frac{\partial \rho_1}{\partial t} = -\rho_0 \nabla \cdot \boldsymbol{v}_1 - v_{1z} \frac{\partial \rho_0}{\partial z} = -\rho_0 \nabla \cdot \boldsymbol{v}_1 + \rho_0 v_{1z} \frac{g}{c_0^2}, \tag{48}$$

linearized momentum equation

$$\frac{\partial \boldsymbol{v}_1}{\partial t} = -\frac{1}{\rho_0} \nabla p_1 - \frac{\rho_1}{\rho_0} g\hat{\boldsymbol{z}}, \tag{49}$$

and energy equation

$$\begin{aligned} \frac{\partial p_1}{\partial t} &= -\gamma p_0 \nabla \cdot \boldsymbol{v}_1 + \rho_0 g v_{1z} + \nabla \cdot \left[D_0 \nabla p_1 - D_0 \frac{\rho_1}{\rho_0} \nabla p_0 \right] \\ &= -\gamma p_0 \nabla \cdot \boldsymbol{v}_1 + \rho_0 g v_{1z} + D_0 \nabla^2 p_1 + \frac{D_0 g}{c_0^2} \frac{\partial p_1}{\partial z} + D_0 g \frac{\partial \rho_1}{\partial z} + D_0 N_0^2 \rho_1 . \end{aligned} \tag{50}$$

The added degrees of freedom stabilize the atmosphere. Linearization of equations (48)–(50) with the WKB *Ansatz* yields the dispersion relation

$$\frac{k^2 c_s^2 + N_0^2}{\omega^2} - (\gamma - 1) \frac{k_\perp^2 g}{\omega^4} - i \frac{k^2 D_0}{\omega} - \frac{k_\parallel g D_0}{c_0^2 \omega} + 2i \frac{k_\perp^2 D_0 N_0^2}{\omega^3} + \frac{k_\perp^2 D_0 k_\parallel g}{\omega^3} = 1 . \tag{51}$$

Normalization of ω to N_0 puts equation (51) in the form

$$\left(\frac{\omega}{N_0}\right)^4 + M_0 kh(\cos\theta + ikh)\left(\frac{\omega}{N_0}\right)^3 - [1 + \gamma(kh)^2]\left(\frac{\omega}{N_0}\right)^2 - 2iM_0(kh \sin\theta)^2 \frac{\omega}{N_0} + (\gamma - 1)(kh \sin\theta)^2 = 0 \tag{52}$$

In the absence of radiation diffusion ($M_0 = 0$), equation (52) describes acoustic waves (p-modes) and internal gravity waves (g-modes), with

$$\omega^2 = \frac{1}{2}(k^2 c_s^2 + N_0^2)\left\{1 \pm \left[1 - \frac{4(\gamma - 1)(kg \sin\theta)^2}{(k^2 c_s^2 + N_0^2)^2}\right]^{1/2}\right\} \approx \begin{matrix} k^2 c_s^2 + N_0^2 \\ (\gamma - 1)(N_0^2/\gamma) \sin^2\theta \end{matrix} . \tag{53}$$

The approximate forms are valid when $kh \gg 1$, with the upper sign and approximate result appropriate to p-modes, and the lower for g-modes. As is clear from my simplified model, buoyancy is the restoring force for the g-modes.

When radiation diffusion is included, both of these modes are damped. When the damping rate is small compared to the oscillation rate, I find

$$\omega = \pm (N_0^2 + k^2 c_s^2)^{1/2} - \frac{i}{2} k^2 D_0 \tag{54}$$

for the sound waves, and

$$\omega = \pm \left(\frac{\gamma - 1}{\gamma}\right)^{1/2} N_0 \sin\theta - \frac{i}{\gamma} \frac{D_0}{h^2} \sin^2\theta \tag{55}$$

for the internal waves. It is not hard to find the damping rates when these exceed the oscillation rate, but these are of no interest here.

2.3. *Minimum Magnetic Field Strength for Photon Bubble Formation*

The formation of photon bubbles clearly requires the atmosphere to be immersed in a magnetic field strong enough to force the adiabatic work done by a buoyancy oscillation to be entirely due to compression parallel to gravity. I estimate the minimum required strength by supposing the field to be strong enough to allow me to estimate the oscillation frequency and the parallel velocity as a function of the pressure from the one-dimensional theory, while the perpendicular velocity can be estimated from the results in the appendix. From equation (14), the parallel velocity is $v_\parallel = -i\omega h(p_1/p_0)$, while from equation (93), when $\omega^2(1 + B_0^2/4\pi\rho_0 c^2) \ll k^2 v_A^2 = k^2 B_0^2/4\pi\rho_0$, the velocity across the magnetic field is $v_\perp = -\omega(k_\perp/2k^2)\beta_0(p_1/p_0)$. Here

$$\beta_0 \equiv \frac{8\pi p_0}{B_0^2} \tag{56}$$

is the ratio of radiation pressure to magnetic pressure.

Adiabatic decompression of the wave due to sideways motion is unimportant if $|k_\parallel v_\parallel| \gg |k_\perp v_\perp|$, which only occurs when $\beta_0 \ll k_\parallel h(k/k_\perp)^2 = kh \cos\theta/\sin^2\theta$. From equation (40), the photon bubble instability is present only if $kh > (\gamma/M_0) \cot\theta$. Then the

internal waves become unstable entropy waves if the magnetic pressure satisfies

$$\frac{B_0^2}{8\pi} > \frac{M_0}{2\gamma} p_0 \frac{LL_\perp}{L_\parallel^2} . \tag{57}$$

Here $L_\perp$ and $L_\parallel$ are the transverse and parallel dimensions of the bubble, equal to $\pi/k_\perp$ and $\pi/k_\parallel$, respectively, and $L = \pi/k$ with $k = (k_\parallel^2 + k_\perp^2)^{1/2}$. Thus, when the diffusion time over a scale height is long compared to the atmospheric sound crossing time ($M_0 \ll 1$), dynamically insignificant magnetic fields can inhibit the release of local overpressures as internal waves and allow photon bubbles to form. Detailed confirmation of this conclusion can be obtained from the solutions of the dispersion relation derived in the Appendix, which will be presented in a separate paper.

3. POLAR MOUND EQUILIBRIUM

The application which motivated this investigation is the possible formation of photon bubbles in the plasma mounds believed to form at the poles of accreting neutron stars. We need a model of the equilibrium structure of such a mound in order to apply the stability results to this environment. I show here that the exponential atmosphere accurately captures the essential vertical stratification of steady, laminar flow onto the polar caps of a neutron star, when the opacity controlling the conduction of radiation is constant, as is the case for Thomson scattering.

Consider the simplest possible model of the low-altitude accretion flow onto a strongly magnetized neutron star. Assume the accretion flow falls onto the star within a circular polar flux tube of constant cross-sectional area whose intersection with the stellar surface defines a polar cap of area $A_{\rm cap} = \pi R_*^2 \theta_c^2$, where R_* is the stellar radius ~ 10 km, and θ_c is the opening angle of the polar flux tube as seen from the stellar center. Magnetospheric models suggest $\theta_c \sim 0.1$ for the accretion powered pulsars (see the reviews by Arons et al. 1984, Lamb 1984, and Aly 1986a, b). Assume the flow is steady in the frame corotating with the star, the mass flux in the accretion flow is independent of distance from the central field line of the polar flux tube, and the plasma in the mound sitting on the surface is optically thick to scattering. Above an accretion shock, the plasma is in free-fall, while below the shock, it settles subsonically. Assume the magnetic field is dipolar and the mound height is small compared to $R_*/3$, so that the field can be represented as uniform and vertical with respect to the surface. Finally, assume radiation provides all the pressure needed to support the plasma against gravity. For this geometry, the effective Eddington luminosity is

$$L_{\rm ED}^{\rm (eff)} = \frac{1}{4}\theta_c^2 H_\parallel L_{\rm ED} = \frac{4\pi GMmc}{\sigma_{\rm T}} H_\parallel \frac{\theta_c^2}{4} \sim 10^{35.5} H_\parallel \text{ ergs s}^{-1} , \tag{58}$$

where $H_\parallel = \sigma_{\rm T}/\sigma_{s\parallel}$, $\sigma_{\rm T}$ is the Thomson cross section and $\sigma_{s\parallel}$ is the Rosseland averaged cross section for radiation whose diffusive flux is parallel to B_0. For accretion luminosity onto one pole L_a larger than $L_{\rm ED}^{\rm (eff)}$, the freely falling plasma above the mound is optically thick to scattering in the direction parallel to B_0.

Assume that in the subsonic settling region, the upwards diffusive flux of radiation is exactly balanced by the downward advection of radiative enthalpy, a hypothesis well justified by more detailed calculations (Arons & Klein 1992, in preparation). Then

$$F_{\rm enthalpy} + F_{\rm diffusion} = -4pv - \frac{mc}{\rho\sigma_{s\parallel}} \frac{\partial p}{\partial s} \approx 0 , \tag{59}$$

where ρ is the mass density, v is the speed of the downward directed flow along the superstrong background magnetic field B_0, m is the mean molecular weight and s is the distance along the magnetic field, measured from the stellar surface. Assume $H_\parallel$ is independent of the plasma pressure and density, as is true for Thomson scattering. Because ρv is constant on each field line, equation (59) yields

$$p = p_* f(r_\perp) \exp(-s/h) , \tag{60}$$

where p_* is a constant, $f(r_\perp)$ an arbitrary function of distance from the central field line, and

$$h = \frac{cm}{4\rho v \sigma_{s\parallel}} = \frac{H_\parallel}{4}\lambda_{\rm T}\frac{c}{v} = \frac{1}{4}\frac{L_{\rm ED}^{\rm (eff)}}{L_a} R_* , \tag{61}$$

where $L_a = GM\dot{M}/R_*$ is the accretion luminosity of one pole and $\lambda_{\rm T}$ is the mean free path for Thomson scattering. The first form of equation (61) is the standard consequence of the balance of diffusion with advection, while the second form is a consequence of steady flow with mass flux independent of distance from the central field line. If the mass flux were to vary with position across the flow, the vertical scale height would also depend on distance from the flow axis.

In order to find the transverse structure of the flow, consider the plasma element located between height s and $s + \Delta s$ within the flow tube of radius $r_\perp$ with cross-sectional area $A(r_\perp) = \pi r_\perp^2$ shown in Figure 4. This fluid element has mass $\Delta M = \rho A(r_\perp)\Delta s$ and releases the gravitational energy $\Delta M g\, \Delta s = \rho A(r_\perp)(GM/R_*^2)\Delta s^2$ as it settles through Δs. Since the net radiative energy flux parallel to B_0 vanishes, the energy released must be lost by photon diffusion across the magnetic field. Let the transverse radiative energy flux be $F_\perp$. During the settling time Δt, the gravitational energy released by the matter between the axis and $r_\perp$ is

$$(2\pi r_\perp \Delta s) F_\perp \Delta t = \Delta M g\, \Delta s = (\pi \rho r_\perp^2 \Delta s)\frac{GM}{R_*^2}\Delta s . \tag{62}$$

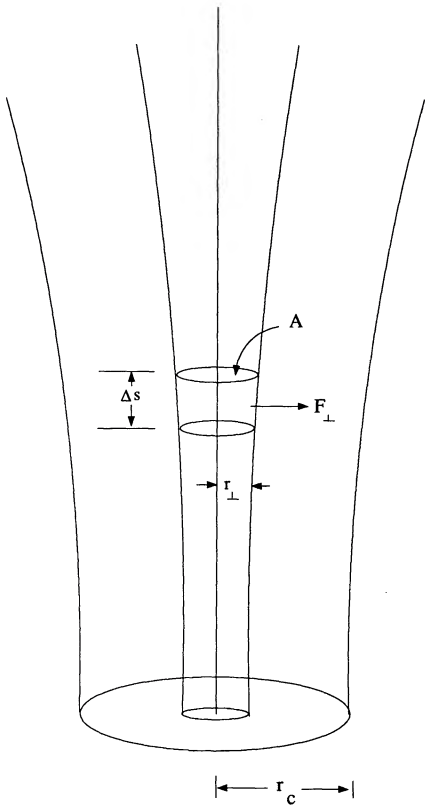

FIG. 4.—Geometry of a settling fluid element. The fluid element's height is Δs and its cylindrical radius with respect to the magnetic axis is $r_\perp$. The transverse flux $F_\perp$ carries away the gravitational energy liberated by settling from s to $s - \Delta s$, with the radiation flowing across the transverse area $2\pi r_\perp \Delta s$ of the fluid element.

Therefore,

$$F_\perp = \frac{1}{2}\left(\rho \frac{\Delta s}{\Delta t}\right)\frac{GM}{R_*^2} r_\perp = \frac{L_a}{2\pi R_*^2 \theta_c}\frac{r_\perp}{r_c}, \tag{63}$$

where we used $v = \Delta s/\Delta t$ and the radius of the polar flux tube $r_c = \theta_c R_*$ in finding the last form of equation (63). Since the energy is lost by radiative diffusion,

$$F_\perp = -\frac{mc}{\rho\sigma_T} H_\perp \frac{\partial p}{\partial r_\perp} = -\frac{mc}{\rho\sigma_T} H_\perp p_* e^{-s/h}\frac{\partial f}{\partial r_\perp}. \tag{64}$$

The flow in the mound is subsonic. Therefore,

$$\rho = -\frac{1}{g}\frac{\partial p}{\partial s} = \frac{p}{gh} = \frac{p_*}{gh} e^{-s/h} f(r_\perp), \tag{65}$$

and

$$\frac{1}{f}\frac{\partial f}{\partial r_\perp} = -\frac{L_a}{2\pi R_*^2 \theta_c}\frac{\sigma_T}{mcgh}\frac{r_\perp}{r_c} = -\left(\frac{L_a}{L_1}\right)^2 \frac{2r_\perp}{r_c}, \tag{66}$$

where

$$L_1 \equiv \frac{L_{ED}^{(eff)}}{\theta_c}\left(\frac{H_\perp}{H_\parallel}\right)^{1/2} = \frac{\theta_c}{4} L_{ED}\sqrt{H_\parallel H_\perp} \sim 3 \times 10^{36}\frac{\theta_c}{0.1}\frac{M_*}{1\ M_\odot}\sqrt{H_\parallel H_\perp}\ \text{ergs s}^{-1}. \tag{67}$$

When $L_a > L_1$, the free-fall *above* the mound is optically thick to scattering in the direction across the magnetic field. Integration of equation (66) yields the radiation pressure

$$p = p_* \exp\left(\frac{-s}{h}\right)\exp\left[\left(\frac{L_a}{L_1}\right)^2\left(1 - \frac{r_\perp^2}{r_c^2}\right)\right]. \tag{68}$$

Thus, the transverse scale of the plasma, which determines the rate of diffusive energy flow across the magnetic field, is

$$h_\perp = \min\left[r_c, \frac{r_c}{2}\left(\frac{L_1}{L_a}\right)^2\right]. \tag{69}$$

When the free-fall is optically thick across B, the transverse scale is small compared to the flow's width.

The solution is complete once we determine the constant p_*. The free-fall is terminated by an accretion shock, which I assume is mediated by radiation conduction (Basko & Sunyaev 1976). The thickness of the shock is $\sim H_\parallel \lambda_T(c/v_{ff})$, where v_{ff} is the free-fall speed. This thickness is comparable to the scale height of the subsonic stratified mound below the shock. Therefore, it is not possible to apply the standard shock jump conditions (Zel'dovich & Raizier 1966) to determine the pressure at the top of the mound on any given field line, even though the shock is thin compared to the mound's *height*; it is not thin compared to the mound's pressure scale height. Instead, a detailed fluid model of the shock structure (Arons & Klein 1992, in preparation) including both gravity and the loss of radiation from the curved shock front due to sideways diffusion shows that at the nominal height of the shock, the radiation pressure of the mound must be set equal to the dynamic pressure of the free fall; in essence, the first few scale heights of the mound must be included into the shock structure itself. At the edge of the flow, where $r_\perp = r_c$, setting the ram pressure equal to the radiation pressure yields

$$p_* = 2\frac{L_a}{\pi R_*^2 \theta_c^2 v_{ff}(R_*)} = 4\times 10^{16} L_{a,37} M_{*,\odot}^{-1/2} R_{*,10}^{3/2}\left(\frac{0.1}{\theta_c}\right)^2 \text{ dynes cm}^{-2}. \tag{70}$$

Here $M_{*,\odot} = M_*/M_\odot$, $L_{a,37} = L_a/10^{37}$ ergs s^{-1}, and $R_{*,10} = R_*/10$ km. For $0 \le r_\perp < r_c$, the equality between the ram and radiation pressure yields the nominal location of the shock to be at the height

$$h_s = R_*\frac{L_a}{L_{ED} H_\parallel}\left(1-\frac{r_\perp^2}{r_c^2}\right) = \frac{1}{4}\theta_c R_* \frac{L_a}{L_1}\left(\frac{H_\perp}{H_\parallel}\right)^{1/2}\left(1-\frac{r_\perp^2}{r_c^2}\right). \tag{71}$$

Thus the mound's height becomes comparable to its radius at accretion luminosities a few times L_1, since $H_\perp/H_\parallel \sim 1$ (Arons et al. 1987). For luminosities comparable to L_{ED}, equation (71) implies the peak of the mound would be a full *stellar* radius. On the other hand, since

$$h_s(r_\perp = 0) = \left(\frac{L_a}{L_1}\right)^2 h, \tag{72}$$

the shock stands many scale heights above the surface only when $L_a \gg L_1$. Indeed, since the shock has a thickness comparable to h, the shock exists as a thin transition layer only for accretion luminosities larger than L_1. For lower luminosities, gravitational stratification of the deceleration region is unimportant.

The density in the mound is now obtained from the condition of approximate hydrostatic equilibrium (eq. [65]). The result is

$$\rho = \rho_* \exp\left(\frac{-s}{h}\right)\exp\left[\left(\frac{L_1}{L_a}\right)^2\left(1-\frac{r_\perp^2}{r_c^2}\right)\right], \tag{73}$$

with the base density

$$\rho_* \equiv \frac{p_*}{gh} = \frac{3m}{\pi R_* r_e^2}\frac{c}{v_{ff}(R_*)}\left[\frac{L_a}{L_{ED}^{(eff)}}\right]^2 = 3\times 10^{-5}(M_{*,\odot} R_{*,10})^{-1/2}\left[\frac{L_a}{L_{ED}^{(eff)}}\right]^2 \text{ g cm}^{-3}$$

$$= 3\times 10^{-2} L_{a,37}^2 M_{*,\odot}^{-5/2} R_{*,10}^{-1/2}\left(\frac{0.1}{\theta_c}\right)^4 H_\parallel^{-2} \text{ g cm}^{-3}. \tag{74}$$

Here, r_e is the classical radius of an electron. Therefore, the mound has a constant sound speed

$$c_0 = \left(\frac{\partial p_0}{\partial \rho_0}\right)^{1/2} = \frac{v_{ff}(R_*)}{2^{3/2}}\left[\frac{L_{ED}^{(eff)}}{L_a}\right]^{1/2} = 10^4 M_{*,\odot} R_{*,10}^{-1/2}\left(\frac{\theta_c}{0.1}\right) H_\parallel^{1/2} L_{a,37}^{-1/2} \text{ km s}^{-1}. \tag{75}$$

The Thomson optical depth of this mound structure is large, both along and across the magnetic field, when $L_a \gg L_{ED}^{(eff)}$. The Thomson depth from the base of the mound to the shock wave as measured along the central field line is

$$\tau_{T\parallel} = 2(L_a/L_{ED}^{(eff)})[c/v_{ff}(R_*)]\exp[(L_a/L_1)^2],$$

while the Thomson depth from the center of the mound to its edge, measured at the mound's base, is $\tau_{T\perp} = (8/\sqrt{\pi})\tau_{T\parallel}$. These optical depths apply to pure hydrogen; for a cosmic composition, the factor of 2 in the parallel optical depth is replaced by 2.4. By comparison, the scattering optical depth of free-fall all the way to the surface is $\tau_{Tff\parallel} = (2/3)[L_a/L_{ED}^{(eff)}][c/v_{ff}(R_*)]$, while the scattering optical depth across the base of a plasma falling freely onto the cap is $\tau_{Tff\perp} = (L_a/L_1)[c/v_{ff}(R_*)]$. Thus, the surface density of the mound in each direction exceeds that of the overlying free-fall by the factor $\exp[(L_a/L_1)^2]$.

My basic results for the mound (eqs. [68] and [73]) depend on constancy of the ratios of the Rosseland-averaged photon scattering cross sections to the Thomson opacity. In fact, $H_\perp$ and $H_\parallel$ are approximately equal functions of temperature, varying from unity when the radiation temperature T_γ exceeds $T_c \sim \hbar\Omega_{ce}/3$ to 0.2 when the temperature is less than $T_\gamma < T_c/3$ (Arons et al. 1987). Within the mound, radiation is well thermalized (see Burnard, Arons, & Klein 1991 for a detailed study of the thermalization

of radiation in this mound model), with $T_\gamma \propto p^{1/4}$. For fiducial parameters $B \sim 10^{12}$ G, $\theta_c \sim 0.1$, most of the mound plasma occupies the unmodified Thomson scattering regime $T_\gamma > T_c$ when $L_a \gtrsim L_1$. Thus, $H_\perp \approx H_\parallel \approx 1$ is a good approximation over most of the mound's volume for the majority of the known accretion powered pulsars.

Since the mound is highly optically thick and thermalized, the photons which eventually carry away the accretion energy are emitted within this region. However, only a fraction $h_s/R_* \sim L_a/L_{\rm ED}$ of the accretion energy is released in the subsonic region, which is generally much less than the total accretion energy available. Most of the energy is actually released in the shock, whose optical depth is expected to be several $c/v_{\rm ff} \sim 5$–10. The plasma in the shock is unable to thermalize the radiation, but it can energize the photons diffusing into it from the underlying mound through Comptonization. Thus, the slowly settling mound forms the back-lighting photons source for a relatively thin, high-velocity layer from where the observed spectrum is formed. It is known that backlit *static* slabs of plasma in a strong magnetic field with Thomson optical depth in the range of 5–10 are a reasonable model for the spectra of X-ray pulsars (Meszaros & Nagel 1985). It remains to be seen if multicomponent dynamical model suggested here and also discussed by Burnard et al. (1991) yields as good a description of the spectra.

It is not my intent here to comment in detail on the relation of this solution to previous attempts to model the flow structure of polar accretion mounds, since this is addressed elsewhere (Arons & Klein 1992, in preparation) where we also show how this "isothermal" structure arises without making the *Ansatz* (eq. [59]). However, two remarks are in order. First, the basic solution is the same as that found by Kirk (1985), who made essentially the same geometric simplifications. The derivation here relies directly on the conservation of radiative energy, which makes clear that the result does not depend only on a peculiar separation of variables technique. My result differs from Kirk's (1985) in the upper boundary condition, since he did not investigate the connection of the mound to a radiation conduction shock. Instead, he assumed the presence of an optically thin collisionless shock, which leads to different conclusions concerning the mound's height, shape, and base pressure at the outer edge p_*. While a collisionless shock may be embedded in the radiative shock structure, the radiation conduction shock is still present so long as $L_a \gg L_{\rm ED}^{\rm (eff)}$ (Arons & Klein 1992, in preparation). Since this inequality is met for almost all the X-ray pulsars, the mound model described here would be the correct one, if the flow were steady (and if the other geometric simplifications are met, of course).

Second, both of these models differ drastically from that proposed by Basko & Sunyaev (1976) and explored numerically by Braun & Yahel (1984). These authors simplified the intrinsically multidimensional structure of the flow by assuming the transverse scale length of the plasma is *always* equal to the width of the flow channel $\theta_c R_*$. For a given energy density, this assumption fixes the radiation flux across the magnetic field to be $F_\perp \approx Dp_\gamma/\theta_c R_*$. From equation (69), it is clear that this flux underestimates the true value by a factor $\sim(L_1/L_a)^2$ when the free-fall is optically thick across the magnetic field. As a result, Basko & Sunyaev (1976) concluded that almost all the radiation is carried into the star, a result which led to their conclusion that there is an upper limit to the hard X-ray luminosity of an accreting magnetized neutron star. For high-luminosity flows, my results show that this conclusion is an incorrect artifact of their one-dimensionalizing approximation. This same discrepancy between the assumed and true values of $h_\perp$ led to the inability of Braun & Yahel (1984) to find high luminosity, steady flow solutions.

4. PHOTON BUBBLE INSTABILITY OF ACCRETION MOUNDS

If steady flow were a realistic assumption, the finite magnetic pressure at the base of the column would form the limit to steady laminar flow models of polar cap accretion, since

$$p(s = 0, r_\perp = 0) = p_* \exp\left[(L_a/L_1)^2\right] . \tag{76}$$

While $p_* \sim 10^{16.5} L_{a,37}$ dynes cm^2, the base pressure at the mound *surface* just behind the shock, is much less than the magnxtic pressure $p_B = 1.6 \times 10^{22} B_{12}^2$ dynes cm^2, with $B_{12}/10^{12}$ G, the central pressure at the base (eq. [76]) exceeds the confining magnetic pressure, for

$$(L_a/L_1)^2 > 16 + \ln\left[B_{12}^2 M_{*,\odot}^{1/2} L_{a,37}^{-1} R_{*,10}^{-3/2} (\theta_c/0.1)^2\right] .$$

Thus, when L_a exceeds $10^{37.1}$ ergs s^{-1}, magnetic confinement of the mound's deep interior fails. This confinement limit, which is small compared to the luminosities of several accretion-powered pulsars, depends on the parameters only through the square root of the log of the parameters, because of the strong Guassian dependence of the central pressure on the accretion luminosity. While loss of magnetic confinement at the base of the central field line alone probably does not much alter the mound structure, only small increases of the accretion luminosity above this confinement limit cause the high-pressure region to spread through most of the volume of the mound, thus completely altering the equilibrium. One could draw the conclusion that flow in the accretion mounds of high-luminosity sources occurs in a largely field-free region, with the magnetic field largely excluded by the diamagnetic accreted plasma, yet still able to confine the mound because the compressed and stretched field lines are rooted in the crust. Feeding the mound would then require some means of transporting accreting plasma across the highly magnetized, low-pressure skin of the mound into the mound's unmagnetized interior. Quite apart from questions of stability of such a configuration, however, the finite yield strength of the crust (Ruderman 1972) limits the pressure that can be contained to perhaps 10^{26} dynes cm^{-2}, which only marginally increases the confinement limit. Therefore, *laminar* steady flow accretion models onto the polar regions of magnetized neutron stars do not apply to the brighter X-ray pulsars.

The origin of this conundrum lies in the assumed steadiness of the flow. If the medium were to break up into regions where the radiation could flow out with a macroscopic speed large compared to the diffusion speed, the pressure would never build up to the extreme levels implied by equation (76). In this section, I use the equilibrium discussed in § 3 and the stability results derived in § 2 to show that accretion mounds are likely to form radiation filled regions of lowered density which can rise through the settling plasma.

The instability analysis applies to a plane parallel atmosphere, while the mound has pressure and density stratified across the magnetic field with a typical scale length $r_c(L_1/L_a)^2$. The growth rates derived therefore refer to bubbles of small transverse extent,

$L_\perp < \pi r_c (L_1/L_a)^2$. The sound speed c_0 and the vertical scale height of the mound are constants, as was assumed in the stability analysis.

The stability analysis also assumes the atmosphere to be static, while in the accretion mound, the plasma settles subsonically with velocity $\boldsymbol{v}_0 = -v_0(z, r_\perp)\hat{\boldsymbol{e}}_z$. It is straightforward to show that subsonic motion parallel to $\boldsymbol{g}$ and $\boldsymbol{B}_0$ does not affect the growth rate, to lowest order in v_0/c_0. The real part of the frequency is affected by the simple Doppler shift $\omega \rightarrow \omega + k_\parallel v_0$.

The magnitude of the growth rate and of the frequency depends on the ratio of the time it takes a sound wave to cross a vertical scale height to the time it takes photons to diffuse through a scale height. This ratio is the parameter M_0 defined in equation (11). From equation (61), equation (11) yields

$$M_0 = 4\frac{v_0}{c_0} = 4\sqrt{\frac{3}{4}}\,M_s\,, \tag{77}$$

where M_s is the total acoustic Mach number based on the adiabatic sound speed $c_s = (4p_0/3\rho_0)^{1/2}$.

The oscillation frequency of an overstable photon bubble is then

$$\omega \simeq -k_\parallel v_0 - N_0 M_0 \frac{k_\parallel h(k_\perp h)^2}{1 + \gamma(k_\parallel h)^2}\,. \tag{78}$$

An individual bubble of fixed width $L_\perp = \pi/k_\perp$ moves along the magnetic field with the group velocity

$$v_g = \frac{\partial\omega}{\partial k_\parallel} \approx -v_0 + \frac{v_d}{\gamma}\left(\frac{\pi}{k_\parallel L_\perp}\right)^2\,, \tag{79}$$

where the diffusion speed is $v_d = c_0 M_0 = D_0/h$. The bubble motion is always upward in the frame of the fluid. From equation (77), the diffusion speed in the settling mound is $v_d = 4v_0$, and maximum growth occurs for bubbles with $k_\parallel L_\perp \ll 1$. Therefore, my diffusion-advection model of polar cap structure predicts that bubbles will form which move up both in the frame of the fluid and in the frame of the neutron star, with rise speed some multiple of the photon diffusion velocity, *not* with the buoyancy velocity $\sim(gL_\perp)^{1/2}$ assumed by Spiegel (1977). This difference occurs because the bubbles are energetically open and move because the exchange of heat with the surroundings is needed to maintain the buoyancy, in contrast to the buoyancy of a permanent bubble in a Rayleigh-Taylor unstable medium.

An example will illustrate the orders of magnitude involved. Consider uniform flow with accretion luminosity onto one pole $L_a = 1 \times 10^{37}$ ergs s^{-1}. Assume the star has $M_* = 1\ M_\odot$, $\theta_c = 0.1$ and $R_* = 10$ km. The polar cap has a diameter of 2 km. The simple mound model yields a vertical scale height $h = 0.086$ km while the peak of the shock sits at the height $h_s = 0.7$ km above the surface; the mound is almost 8.5 scales heights tall. The transverse scale length of the mound is $h_\perp \approx 0.06$ km. The isothermal sound speed in the mound is $c_0 = 10^4$ km s^{-1}. Since $g = 1.3 \times 10^{14}$ cm s^{-2}, $N_0 = 1.3 \times 10^5$ s^{-1}; an isothermal sound wave crosses a vertical scale height in 7.5 μs. Consider a depth where the infall velocity has dropped to 500 km s^{-1}. From equation (73) and the equation of continuity, this speed occurs about 0.3 km above the surface on the magnetic axis, while from equation (77), $M_0 = 0.2$. Equation (79) suggests that the dominant bubbles will be those which rise the fastest, i.e., have the smallest possible parallel wave number, while the instability analysis applies only to modes which are thin in the transverse direction, $L_\perp/\pi < h_\perp < h$. By taking $k_\perp$ sufficiently large, the threshold condition (40) can be satisfied for $k_\parallel h \sim 1$. Then the photon bubble mode has oscillation frequency

$$\omega \approx -2.6 \times 10^3 k_\parallel h - 6 \times 10^4 (k_\perp h_\perp)^2 \frac{k_\parallel h}{1 + (4/3)(k_\parallel h)^2}\ \text{s}^{-1}\,, \tag{80}$$

corresponding to a maximum oscillation period of around 100 μs. This mode grows rapidly. From equation (45) with $k_\perp \gg k_\parallel$, the growth rate is

$$\Gamma \approx 10^5 k_\perp h_\perp\ \text{s}^{-1}\,. \tag{81}$$

Thus, the bubble grows 10 times as fast as it oscillates.

The nonlinear fate of these vertical "fingers" of radiation is not readily discerned from the linear theory. If the bubbles were to remain isolated, their small scale ($kh \gg 1$) suggests that they would cause relatively small fluctuations in the emergent luminosity, as they rise and burst at the surface of the flow (Prendergast & Spiegel 1973). However, the fact that bubbles with long wavelength parallel to the magnetic field have a larger group speed suggests long bubbles will overtake and merge with small ones, leading to coalescence. This sort of behavior is consistent with the larger scale structures apparent in the numerical simulations described by Klein & Arons (1989, 1991), in which large-scale bubbles begin to appear within 100 μs. If coalescence is the final fate of photon bubbles, the flow can become dominated by one or a few large-scale bubbles, whose expansion to optical depth unity in the accretion flow would give large-scale fluctuations, forming either a limit cycle or chaos in the emergent luminosity. Further investigation of the relation between the linear theory and the final state of photon bubbles will be described elsewhere (Klein & Arons 1992, in preparation).

5. CONCLUSIONS

5.1. *Comparison with Other Stability Results*

Apart from speculations on the existence of photon bubbles and on their possible astrophysical significance, the main previous study of photon bubble formation in the isothermal atmosphere is in the unpublished Ph.D. dissertation of Marzek (1977). He showed that in the *unmagnetized* isothermal atmosphere, both sound waves and g-modes are stable, even when true absorption is

neglected; including absorption only enhances the stability. As explained in § 3, a vertical magnetic field with energy density exceeding $p_{\rm rad}[t_s(h)/t_d(h)]$ must be present if the instability is to occur, so it is no surprise that Marzek did not find photon bubbles in his stability analysis. Here t_s and t_d are, respectively, the sound crossing and photon diffusion times for the specified length scale, and $h = c_0^2/g$ is the scale height of the isothermal atmosphere.

Syrovatskii & Zhugzhda (1967) showed that overstable compressible *convection* appears in the sound waves in a strongly magnetized atmosphere whose temperature linearly increases with height, if the ratio of specific heats of the plasma exceeds 1.2. My results, which show that the sound waves are stable, are consistent with theirs, since the model atmosphere studied here is isothermal. Hameury et al. (1980) studied the same sort of plane parallel atmosphere as that used by Syrovatskii & Zhugzhda (1967), with radiative energy density (and entropy) increasing linearly with height, and found essentially the same *convective* results by a fully numerical method. Wang (1982) studied the same type of model. He also found instability but with results differing in quantitative detail; the origin of the differences is unclear.

Thus, previous calculations either found stability, or, when the magnetic field is strong, found overstable convection rather than photon bubbles when the underlying model has temperature *increasing* with height. It is perhaps not surprising that systems with inverted entropy gradients can form overstable compressible motions along the magnetic field, since in the absence of strong magnetic fields, they would show a Rayleigh-Taylor instability. In circumstances where the radiative entropy is stably stratified with respect to interchange motions, the results presented here are the first to show that gravitationally bound atmospheres can still form density depeleted regions through conductively driven overstability of the entropy mode (i.e., of the internal waves), when the magnetic field is sufficiently strong. I have used a simple accretion model to suggest that polar accretion mounds on neutron stars, supported against gravity by radiation pressure and confined in the transverse directions by the vertical magnetic field, do have *convectively* stable structure yet can form photon bubbles on the 100 μs to 1 ms time scale.

Recently Hogan (1991), in the context of the formation of density inhomogeneities in the early universe, has argued that "mock gravity," due to shadowing of the radiative force on a particle through absorption of the photons by other particles, might lead to the formation of density depleted regions analogous to the photon bubbles first suggested by Prendergast & Spiegel (1973), even in an unmagnetized medium. His conclusion is not consistent with mine or Marzek's (1977). He found instability because he studied the instability of pressure-free dust, as it absorbs radiation. This model neglects the stabilizing effect of the small but non-zero adiabatic expansion in the internal waves which are the basic unstable modes in a *gas* acted upon by the mock gravitational field. Thus Hogan's (1991) instability is not germane to the formation of photon bubbles in high-temperature plasmas.

5.2. *Summary and Speculations*

In this paper, I have shown that an isothermal, plane-stratified, magnetized scattering atmosphere which is supported against gravity by radiation pressure is overstable with respect to the formation of elongated vertical fingers of low-density plasma which are filled by radiation, even though the atmosphere is stable to convective and to interchange ("Rayleigh-Taylor") motions. Expression (40) is the basic stability criterion, while expression (42) gives the oscillation period of unstable waves whose wavelength satisfies the stability criterion; expression (43) gives an approximation to the growth rate of the unstable bubbles found by numerical solution of the dispersion relation (33). These results are valid when $t_s(h) \ll t_d(h)$. The unstable bubbles have a ratio of vertical length to transverse width of $L_{\|}/L_{\perp} \sim 1.4[t_d(h)/t_s(h)]^{1/2}$ when in the linear phase. The photon bubbles appear as an instability of the entropy mode in the strongly magnetized plasma, which in turn is the degenerate limit of the internal gravity waves (g-modes). The transport of heat out of high radiation pressure regions and into low-pressure zones in the direction orthogonal to gravity and the magnetic field causes the wave to propagate; the instability arises from the net transport of heat along the magnetic field which always acts to carry heat from high-density to low-density regions, as is shown by expression (23).

I also outlined a simple model of a settling accretion mound on the surface of a neutron star. The basic results of this model are contained in expressions (68) and (70) for the radiation pressure, and expressions (73) and (74) for the mass density. From this model, I concluded that polar mounds of accreting magnetized neutron stars are likely to be subject to the formation of photon bubbles, and I used the stability results to suggest that the bubbles would coalesce and form large-scale fluctuations in the luminosity, as is consistent with the numerical results outlined by Klein & Arons (1989, 1991, and 1992 in preparation).

It is beyond the scope of this paper to discuss the consequences of this instability for models of neutron star accretion in detail. Expression (79) shows that larger bubbles might be expected to rise faster than small ones, a phenomenon common to buoyancy driven motions. Thus, as remarked above, one expects the nonlinear development to be dominated by a small number of large bubbles, a conclusion consistent with the preliminary numerical simulations of the phenomenon (Klein & Arons 1989, 1991). The nonlinear consequences of these large bubbles might involve bubble rise until they reach optical depth unity in the overyling free-fall, where the radiation abruptly leaks out (the bubbles "burst") and the plasma halted above the bubbles falls down. This outcome would produce large amplitude limit cycles in the X-ray luminosity on the 1–10 ms time scale, and would be of relevance to short time variability in accretion powered pulsars for which detailed observational searches have not yet been mounted. Since the luminosity is locally super-Eddington, the bubbles might also have enough momentum to expel all the overlying plasma, which would lead to a limit cycle time scale controlled by the time for the exterior flow to refill the magnetosphere (≥ 1 s for accretion powered pulsars, ≥ 100 ms for weakly magnetized neutron stars in low-mass X-ray binaries). If this phenomenon occurs, it may be relevant to the temporal fluctuations of the Rapid Burster (Lewin et al. 1976) and of low mass X-ray binaries which show quasi-periodic oscillations (e.g., van der Klis et al. 1985) in their light curves. Construction of models along these lines requires the deeper knowledge of the nonlinear fate of photon bubbles which will be provided by studies now in progress (Klein & Arons 1992, in preparation).

Special thanks are due to Ed Spiegel, for providing me with a copy of C. J. Marzek's dissertation, and for entertaining discussions of "photohydrodynamic" stability and other less technical topics. I am also indebted to Richard Klein for his comments on the

relation between the results described here and our numerical simulations of polar column flow. This work was supported in part by NSF grant no. AST-8615816, by NASA Astrophysical Theory grant no. NAGW-2413, and by the institute of Geophysics and Planetary Physics-Lawrence Livermore National Laboratory through grant no. 90-14. Part of the research was done at the Lawrence Livermore National Laboratory under the auspices of the United States Department of Energy, through Contract no. W-7405ENG-48.

APPENDIX

PHOTON BUBBLE DISPERSION RELATION IN A FINITE MAGNETIC FIELD

Here I investigate the photon bubble instability for arbitrary magnetic field strength. I assume the magnetic field is uniform and vertical, with $\boldsymbol{B}_0$ either parallel or antiparallel to $\boldsymbol{g}$. The continuity and energy equations are given by equations (48) and (50), respectively, while the equation of motion changes to

$$\rho_0 \frac{\partial \boldsymbol{v}}{\partial t} = -\nabla p_1 - \rho_1 \boldsymbol{g} + \frac{1}{c} \boldsymbol{J} \times \boldsymbol{B}_0. \tag{82}$$

Ampere's law gives

$$\boldsymbol{J} = \frac{c}{4\pi} \nabla \times \boldsymbol{B}_1 - \frac{1}{4\pi} \frac{\partial \boldsymbol{E}}{\partial t}\,; \tag{83}$$

I retain the displacement current, since some environments of interest are embedded in fields so strong that the displacement current can exceed the conduction current, in spite of the low frequencies of interest. I assume ideal MHD is valid. Then

$$\boldsymbol{E} = -\frac{1}{c} \boldsymbol{v}_1 \times \boldsymbol{B}_0\,, \tag{84}$$

and

$$\frac{\partial \boldsymbol{B}_1}{\partial t} = \nabla \times (\boldsymbol{v}_1 \times \boldsymbol{B}_0)\,. \tag{85}$$

The choice of axes in the plane perpendicular to $\boldsymbol{g}$ and to $\boldsymbol{B}_0$ is arbitrary. As in the $B_0 = 0$ and $B_0 = \infty$ cases, I assume a plane wave representation of the disturbances. Then all spatial variation in the plane perpendicular to $\boldsymbol{g}$ and $\boldsymbol{B}_0$ can be assumed to be along the x-axis.

Motion in the y-direction decouples from the flow in the x–z plane. From equation (85), bending of the magnetic field by motion in the y-direction yields

$$\frac{\partial B_{1y}}{\partial t} = B_0 \frac{\partial v_y}{\partial z}\,, \tag{86}$$

while equation (83) yields

$$J_x = -\frac{c}{4\pi} \frac{\partial B_{1y}}{\partial z} + \frac{B_0}{4\pi c} \frac{\partial v_y}{\partial t}\,. \tag{87}$$

Substituting equation (87) into the y-component of equation (82) yields

$$\rho_0 \epsilon_\perp \frac{\partial v_y}{\partial t} = \frac{B_0}{4\pi} \frac{\partial B_{1y}}{\partial z}\,, \tag{88}$$

where

$$\epsilon_\perp \equiv 1 + \frac{B_0^2}{4\pi \rho_0 c^2} \tag{89}$$

measures the "inertia" of the magnetic field contributed by the displacement current. The quantity $\epsilon_\perp$ is closely related the static dielectric function of a magnetized plasma

$$w_\perp \equiv 1 + \frac{4\pi \rho_0 c^2}{B_0^2} = \frac{\epsilon_\perp}{\epsilon_\perp - 1}\,. \tag{90}$$

Differentiating equation (88) once with respect to t and substituting from equation (86) yields the wave equation

$$\frac{\partial^2 v_y}{\partial t^2} - u_A^2 \frac{\partial^2 v_y}{\partial z^2} = 0\,, \tag{91}$$

where the relativistic Alfvén speed is

$$u_A^2 \equiv \frac{c^2}{w_\perp} = \frac{B_0^2}{4\pi\rho_0}\left(1 + \frac{B_0^2}{4\pi\rho_0 c^2}\right)^{-1} . \tag{92}$$

Equation (91) represents the propagation of the usual incompressible Alfvén wave, and shows that this mode is decoupled from the pressure disturbances which form photon bubbles.

Perpendicular motions in the x-direction yield magnetic disturbances which can alter the total pressure and therefore affect the propagation of both sound and internal waves, and therefore of photon bubbles. Use of the WKB *Ansatz* (eq. [28]) in the continuity equation (48), the x- and z-components of the equation of motion (eq. [82]), the x- and z-components of the Faraday law (eq. [85]) and the y-component of equation (83), yields

$$\frac{\hat{B}_{1\parallel}}{B_0} = \frac{k_\perp^2 c_0^2}{\omega^2 \epsilon_\perp D_m}\frac{\hat{p}_1}{p_0} , \qquad \frac{\hat{B}_{1\perp}}{B_0} = -\frac{k_\parallel k_\perp c_0^2}{\omega^2 \epsilon_\perp D_m}\frac{\hat{p}_1}{p_0} , \tag{93}$$

$$\hat{v}_{1\parallel} = \frac{c_0^2}{\omega D_\rho}\left[k_\parallel - i\frac{k_\perp^2 g}{\omega^2 D_m \epsilon_\perp}\right]\frac{\hat{p}_1}{p_0} , \qquad \hat{v}_{1\perp} = \frac{k_\perp c_0^2}{\omega \epsilon_\perp D_m}\frac{\hat{p}_1}{p_0} , \tag{94}$$

$$\hat{J}_{1x} = 0 , \qquad \hat{J}_{1y} = -i\frac{ck_\perp}{4\pi} B_0 \frac{(kc_0/\omega)^2}{D_m \epsilon_\perp}\left(1 - \frac{\omega^2}{c^2 k^2}\right)\frac{\hat{p}_1}{p_0} , \qquad \hat{J}_{1z} = 0 \tag{95}$$

and

$$\frac{\hat{p}_1}{\rho_0} = \frac{1}{D_\rho \omega^2}\left[c_0^2\left(k_\parallel^2 + \frac{k_\perp^2}{D_m \epsilon_\perp}\right) + ik_\parallel g\right]\frac{\hat{p}_1}{p_0} . \tag{96}$$

Here

$$D_\rho \equiv 1 + i\frac{k_\parallel g}{\omega^2} - \frac{N_0^2}{\omega^2} , \tag{97}$$

and

$$D_m \equiv 1 - \frac{k^2 u_A^2}{\omega^2} . \tag{98}$$

The pressure remains related to the velocity and density through the energy equation (50). The WKB *Ansatz* in this equation yields

$$D_p \frac{\hat{p}_1}{p_0} = i\frac{g v_\parallel}{\omega c_0^2} + \gamma\frac{\boldsymbol{k}\cdot\boldsymbol{v}}{\omega} + i\frac{D_0}{\omega c_0^2}(N_0^2 + ik_\parallel g)\frac{\hat{\rho}_1}{\rho_0} , \tag{99}$$

with

$$D_p \equiv 1 + i\frac{k^2 D_0}{\omega} + \frac{D_0 k_\parallel g}{c_0^2 \omega} . \tag{100}$$

I find the dispersion relation by substituting the velocity and density amplitudes from equation (93) into equation (99); a useful trick is to evaluate $\boldsymbol{k}\cdot\boldsymbol{v}$ from the continuity equation rather than working it out directly. The result is

$$\frac{k_\parallel^2 c_s^2 + N_0^2}{\omega^2} - i\frac{k^2 D_0}{\omega} - \frac{k_\parallel g D_0}{c_0^2 \omega} + i\frac{k_\perp^2 D_0 N_0^2}{\omega^3} + \frac{k_\perp^2 D_0 k_\parallel g}{\omega^3} + \frac{1}{\epsilon_\perp D_m}\left[\frac{k_\perp^2 c_s^2}{\omega^2} - (\gamma - 1)\frac{k_\perp^2 g}{\omega^4} + i\frac{k_\perp^2 D_0 N_0^2}{\omega^3} - \frac{k_\perp^2 D_0 k_\parallel g}{\omega^3}\right] = 1 . \tag{101}$$

Equation (101) reduces to the one-dimensional result (eq. [32]) when $B_0 \to \infty$, while it is equivalent to the three-dimensional result (eq. [51]) when $B_0 \to 0$.

REFERENCES

Aly, J. J. 1986a, in Magnetospheric Phenomena in Astrophysics, ed. R. I. Epstein & W. C. Feldman (New York: AIP), 45
———. 1986b, in Plasma Penetration into Magnetospheres, ed. N. Kylafis, J. Papamastorakis, & J. Ventura (Iraklion: Crete Univ. Press), 125
Arons, J., Burnard, D. J., Klein, R. I., McKee, C. F., Pudritz, R. E., & Lea, S. M. 1984, in High Energy Transients in Astrophysics, ed. S. E. Woosley (New York: AIP), 215
Arons, J., Klein, R. I., & Lea, S. M. 1987, ApJ, 312, 666
Basko, M. M., & Sunyaev, R. A. 1976, MNRAS, 175, 395
Braun, A., & Yahel, R. Z. 1984, ApJ, 278, 349
Burnard, D. J., Arons, J., & Klein, R. I. 1991, ApJ, 367, 575
Cowie, L., Ostriker, J. P., & Stark, A. A. 1978, ApJ, 226, 1041
Demel, V., Morfill, G., & Atmanspacher, H. 1990, ApJ, 354, 616
Hameury, J. M., Bonnazola, S., & Heyvaerts, J. 1980, A&A, 90, 359
Hogan, C. 1991, ApJ, 369, 300
Kirk, J. 1985, A&A, 142, 430
Klein, R. I., & Arons, J. 1989, in Proc. 23d ESLAB Symposium on Two Topics in X-Ray Astronomy, ed. N. E. White & T. D. Guyenne (ESA SP-296), 1, 89
———. 1991, in Stellar Atmospheres Beyond Classical Models, ed. L. Crivellari, I. Hubeny, & D. G. Hummer (Boston: Kluwer), 205
Klein, R. I., Stockman, H. S., & Chevalier, R. A. 1980, ApJ, 237, 912
Lamb, F. K. 1984, in High Energy Transients in Astrophysics, ed. S. E. Woosley (New York: AIP), 179
———. 1989, in Proc. 23d ESLAB Symposium on Two Topics in X-Ray Astronomy, ed. N. E. White & T. D. Guyenne (ESA SP-296), 1
Lewin, W. H. G., et al. 1976, ApJ, 207, L95
Marzek, C. J. 1977, Ph.D. dissertation, Columbia Univ.
Meszaros, P., & Nagel, W. 1985, ApJ, 298, 147

Mihalas, D., & Mihalas, B. W. 1984, Foundations of Radiation Hydrodynamics (New York: Oxford Univ. Press)
Prendergast, K. H., & Spiegel, E. A. 1973, Comments Astrophys Space Phys., 5, 43
Ruderman, M. A. 1972, ARA&A, 10, 452
Spiegel, E. A. 19876, in Colloq. Internat. du CNRS No. 250, Physique des Mouvements dans les Atmosphères Stellaires, ed. R. Cayrel & M. Steinberg (Paris: CNRS), 19
———. 1977, in IAU Colloq. 38, Problems of Stellar Convection, ed. E. A. Spiegel & J.-P. Zahn (Berlin: Springer), 267
Syrovatskii, S. I., & Zhugzhda, Yu. D. 1967, AZ, 44, 1180 (Soviet Astronomy—AJ, 11, 945)
Thomas, L. H. 1930, Quart, J. Math., 1, 239
van der Klis, M., Jansen, F., van Paradijs, J., Lewin, W. H. G., Trumper, J., van den Heuvel, E. P. J., & Sztajno, M. 1985, Nature, 316, 225
Weinberg, S. 1971, ApJ, 168, 175
Zel'dovich, Ya. B., & Raizier, Yu. P. 1966, Physics of Shock Waves and High-Temperature Hydrodynamic Phenomena, Vol. 2 (New York: Academic), 543
Zhugzhda, Yu. D. 1970, AZ, 47, 340 (Soviet Astronomy—AJ, 14, 274)